Science and Technology Indonesia
e-ISSN:2580-4391 *p*-ISSN:2580-4405
Vol. 10, No. 1, January 2025

Research Paper

Synthesis and Characterization of Hydroxyapatite Composites Based on Tutut (*Belamya Javanica*) and Magnetite by Coprecipitation as Adsorbents of Pb Metals Ion

Charlena[1*], Nazriati[2], Betty Marita Soebrata[1], Muhammad Dicky Iswara[1]

[1]*Department of Chemistry, Faculty of Mathematics and Natural Sciences, Bogor Agricultural Institute, Bogor, 16680, Indonesia*
[2]*Department of Chemistry, Faculty of Mathematics and Natural Sciences, The State University of Malang, Malang, 65145, Indonesia*
***Corresponding author**: charlena@apps.ipb.ac.id

Abstract
Increased industrial activity can result in the emission of pollutants into the environment, such as heavy metals, which are a significant source of concern. A practical approach to reduce this problem is to utilize Pb metal adsorption. This study aims to synthesize HAp from *Bellamya javanica* clam shells and characterize the HAp-Fe_3O_4 composite as a Pb metal ion adsorbent. FTIR and XRD analysis results showed the successful fabrication of the composite, resulting in a crystal dimension of 7.63 nm and a crystallinity level of 84.80%. SEM characterization showed a porous structure with a particle size of 10.98 μm. Adsorption studies of Pb(II) ions showed that the HAp-Fe_3O_4 composite efficiently adsorbed Pb(II) ions, with the adsorption efficiency increasing from 95.80% to 98.40%. The adsorption isothermal model of the HAp-Fe_3O_4 composite follows the Freundlich model with a $1/n$ value of 0.31 and a K_F value of 25.35 L/g. The adsorption kinetics study of the HAp-Fe_3O_4 composite follows the pseudo-second-order model with an R^2 value of 1, and the thermodynamic study shows the Gibbs free energy is negative, which indicates that the adsorption process is thermodynamically optimal and spontaneous. In addition, the enthalpy value is positive, indicating that the interaction between the adsorbent and lead ions is endothermic, and the entropy is negative, indicating the reduction of random collisions of lead ions in the solid (adsorbent) and aqueous solution during adsorption.

Keywords
Adsorbents, *Bellamya javanica* Shells, Coprecipitation, Hydroxyapatite, Magnetite

Received: 26 June 2024, Accepted: 28 October 2024
https://doi.org/10.26554/sti.2025.10.1.111-122

1. INTRODUCTION

The growing industry in Indonesia can harm the environment. One possible consequence is decreased water quality, mainly due to heavy metal pollution caused by improper waste disposal. Industries such as metals, electroplating, tanning, textiles, and paints produce waste that contains various hazardous materials that must be treated and disposed of in a specific way to avoid environmental harm. Heavy metals are non-biodegradable, toxic, and can accumulate biologically in the food chain, making them highly harmful contaminants (Murmu et al., 2024). Certain metals, especially in high concentrations, are hazardous if they contaminate water, soil, and air. One type of heavy metal that is very dangerous is lead (Pb). Lead is naturally available in metal ores and widespread volcanic grains (Yan et al., 2022).

Lead metal is classified as a highly toxic compound and is carcinogenic to humans (Mielke et al., 2022). Lead is a silvery grey, malleable metallic substance in a solid state characterized by a melting temperature of 327.43 °C and a boiling temperature of 1740 °C. Lead's hue can diminish when exposed to air (Santucci and Scully, 2020). Lead is very soft and easy to form, so it is easy to melt, shape, and roll. Adsorption is one of the ways that can be done to overcome Pb heavy metal pollution because its ability to absorb makes adsorption one of the effective methods to deal with heavy metal pollution (Vesali-Naseh et al., 2021). Magnetite is a compound that can adsorb heavy metals. Magnetite has the highest magnetic properties among other transition metal oxides. However, due to its single property that is still lacking in adsorbing Pb metal, according to El-Dib et al. (2020), magnetite can only adsorb Pb metal with an adsorption efficiency of 80%, so magnetite needs to be composited with one of the compounds that have better adsorption ability in soaking Pb metal to improve physicochemical and mechanical properties in soaking Pb metal, namely with hydroxyapatite (Noh et al., 2019).

Originating from the monomer calcium apatite ($Ca_{10}(PO_4)_6(OH)_2$), hydroxyapatite is a type of calcium phosphate mineral found in nature. Because of its high hydrophilicity, hydroxyapatite can interact powerfully with polar and ionic molecules,

including ions of heavy metals. It can trap Pb metal with an adsorption efficiency of 89.73% (Wang et al., 2019). Hydroxyapatite-based (HAp) adsorbents can help bind dyes, heavy metals, and other pollutants. Because of its unique properties and makeup, hydroxyapatite can exchange ions, has a restricted solubility in water, can withstand high temperatures, and is highly attracted to various pollutants. The use of hydroxyapatite as a sorbent is becoming more and more common for the removal of multiple contaminants. If natural materials such as *Bellamya javanica* shells are used instead of the more common precursors for calcium and phosphate, the cost of the adsorption process may be reduced.

Belamya javanica is an Operculata species living in shallow waters. Waste from eating snail meat is called shells, and it still needs to be known to utilize this waste commercially. Many minerals, including calcium, are contained in this waste (Ngouoko et al., 2022). Calcium carbonate binds to an organic matrix, a complex protein secreted by the outer epithelium of mollusks in the shell structure as calcite and aragonite crystals. *Bellamya javanica* shell contains a lot of calcium carbonate. Recent research has made significant progress in synthesizing Hydroxyapatite-Iron oxide (HAp-Fe_3O_4) from the shells of field snails, which shows the success of using natural materials to support oxidation and calcium supply. Calcination of calcium carbonate ($CaCO_3$) in the shell produces CaO, the main component of HAp. HAp-Fe_3O_4 composites are synthesized via coprecipitation and have applications in the environmental and medical fields. Rich in calcium carbonate, the shells produce hydroxyapatite (HAp) mixed with magnetite (Fe_3O_4) to improve the quality of adsorption and magnetic materials.

2. EXPERIMENTAL SECTION

2.1 Chemical and Instrument

The researchers used West Java rice snail shells to make the composites. They also included additional chemicals, including $(NH_4)_2HPO_4$ (Merck), $FeCl_2.4H_2O$ (Merck), $FeCl_3.6H_2O$ (Merck), NH_4OH (Merck), HNO_3 (Merck), aquifer, NaOH pellets (Merck), and $Pb(NO_3)_2$ (Merck). The researchers characterized these materials using a variety of instruments, including XRD (PANalytical Aeris Cu-Source), AAS-GFS (Thermo Scientific iCE 3000 Series), FTIR (Hitachi 270-50), and SEM-EDX (Hitachi SU-3500).

2.2 Preparation of *Bellamya javanica* Shells

The researchers removed the snail shells by cleaning them and drying them in the sun for a day. This step aims to remove the water content in the shells during the cleaning process. Furthermore, the shells are ground using a mortar to become powder ($CaCO_3$) and sieved using a 100 mesh sieve to obtain snail shell powder with an average particle size of 100 mesh. The researchers ground the snail shells to a size of 100 mesh and then fired them in a furnace at 1000 °C for 5 hours to obtain CaO (Martinez et al., 2024). This process converts $CaCO_3$ powder into CaO solid, as shown in the following reaction Equation 1:

$$CaCO_3(s) \rightarrow CaO(s) + CO_2(g) \quad (1)$$

In addition, FTIR was used to characterize the calcinated CaO and ascertain the sample's calcium concentration.

2.3 Synthesis of Fe_3O_4

To synthesize Fe_3O_4, the researchers used 3.6780 g of $FeCl_2.4H_2O$ and mixed it with 10.0009 g of $FeCl_3.6H_2O$ in 150 mL of distilled water. The researchers then added NH_4OH to the mixture until the pH of the solution reached ten and shook the mix for ninety minutes at 90 degrees Celsius. After cooling the mixture to room temperature, the researchers separated it from the resulting solid by decantation and rinsing through a channel. Various specimens were acquired and dried in a furnace for two hours at 110 °C. The extracted magnetite specimens are then subjected to FTIR analysis to determine the functional groups present in the magnetite. The following reaction Equation 2 illustrates the production of Fe_3O_4:

$$2FeCl_3(aq) + FeCl_2(aq) + 8NH_4OH(aq) \rightarrow Fe_3O_4(s) + 4H_2O(aq) + 8NH_4Cl(aq) \quad (2)$$

2.4 Synthesis of HAp-Fe_3O_4

The synthesized magnetite is put into a chemical beaker containing 100 mL of aquadest. A total of 2.964 grams of CaO from calcination at 1000 °C, was mixed into a 0.8 M HNO_3 solution and added to the synthetic Fe_3O_4 mixture (Vahdat et al., 2019). This mixture is stirred for 15 minutes. In this mixture, diamonium hydrogen phosphate $(NH_4)_2HPO_4$ was added, weighing as much as 3.1693 grams for the manufacture of HAp 1000 which was dissolved with aqueous water until completely dissolved in 100 mL. Subsequently, the $(NH_4)_2HPO_4$ that has been dissolved is gradually combined with both mixtures (at a Ca/P ratio of 1.67). Up to 30 milliliters of NH_4OH are dripped into this mixture. After two hours of heating at 90 °C, the mixture is cooled to room temperature. After being extracted from the solution, the solids are cleaned with aqueducts to a pH of neutral. The composite obtained after filtration is then heated at a temperature of 110 °C for 2 hours so that pure hydroxyapatite-Fe_3O_4 is obtained. The formation of the HAp-Fe_3O_4 composite is as shown in the following reaction Equation 3:

$$10Ca(NO_3)_2(aq) + 6(NH_4)_2HPO_4(aq) + Fe_3O_4(s) + 8NH_4OH(aq) \rightarrow Ca_{10}(PO_4)_6(OH)_2(s) + Fe_3O_4(s) + 20NH_4(NO_3)(aq) + 6H_2O(l) \quad (3)$$

2.5 Application of HAp-Fe_3O_4 Composite as Metal Ion Pb^{2+}

The adsorption process was carried out by inserting 0.03 g of HAp-Fe_3O_4 composite into a solution of 2, 4, 6, and 8 ppm of $Pb(NO_3)_2$ as much as 10 mL with a pH of 6 and was carried out with the addition of NaOH 0.01 M or HNO_3 0.01 M and

stirred at a speed of 200 rpm for 40 minutes using a vortex (Vahdat et al., 2019). The solution is then separated from the adsorbent and the absorbance is measured using AAS. The concentration with the best adsorption power is characterized by SEM to determine the size and quantity of Pb metal ions that can be adsorbed. The percentage of degradation Pb(II) ion will be calculated using the following Equation 4:

$$\text{Efficiency}(\%) = \frac{(C_0 - C_e)}{C_0} \times 100 \quad (4)$$

After 40 minutes of adsorption, the numbers C_0 and C_t, respectively, indicate the concentrations of Pb(II) ions. We utilized the Freundlich and Langmuir models Equations 5 and 6 to calculate the isotherm adsorption that was being investigated.

$$\frac{1}{Q_e} = \frac{1}{K_L Q_m} \times \frac{1}{C_e} + \frac{1}{Q_m} \quad (5)$$

$$\text{Log}\, Q_e = \text{Log}\, K_F \times \frac{1}{n} + \text{Log}\, C_e \quad (6)$$

3. RESULT AND DISCUSSION

3.1 *Bellamya javanica* Shells CaO Powder

Bellamya javanica snail shells that have been converted into $CaCO_3$ powder, then undergo a calcination process to produce CaO. The term calcination refers to the thermal decomposition of $CaCO_3$ into CaO through exposure to high temperatures to increase the value of dolomite and remove impurities by producing various end products (Hafez et al., 2021). The results of the calcination process show a change in color, a transition from a tanned powder to a fine white powder.

The brown color of the calcined CaO powder indicates that there are still organic compounds in the shell. The transition from brown to white color change arises from a reaction involving the decomposition of $CaCO_3$ compounds into CaO during the calcination process (Diningsih and Rohmawati, 2022). Heat treatment in the calcination process is essential for breaking chemical bonds leading to a state where the bonds become less rigid, allowing atoms to move freely and eventually causing the bonds to break (Saikumari et al., 2021). The weight of *Bellamya javanica* snail shell powder before and after calcination can be seen in Table 1.

The calcined shell undergoes weight reduction and discoloration. The weight loss is the result of the release of filler components such as CO_2 gas, H_2O, and organic substances present in the shell of the *Bellamya javanica*. Color change is associated with modifications in the composition of the filler components that occur during the calcination process. This phenomenon is in line with the findings of Saikumari et al. (2021), in which calcium carbonate compounds heated at 1000 °C turn into white calcium oxide compounds. The release of CO_2 brought on by exposure to high temperatures results in this change.

FTIR (Fourier Transform Infrared) analysis is used to determine the chemical's Ca functional group following the production of CaO compounds (Figure 1). The Ca−O functional group emerged at the top with a wave number of 536 cm^{-1}, according to FTIR analysis. The presence of a CO_3^{2-} function group at a peak of 1431 cm^{-1} and an O−H function group at a peak with a wave number of 3640 cm^{-1} suggests that the calcination products retain $CaCO_3$ and CaO, despite their propensity to convert to $Ca(OH)_2$. Because CaO has hygroscopic properties, CaO compounds that convert to hydroxide compounds are thought to be extremely practical (Mohamed et al., 2021). Hydroxide compounds are formed when CaO compounds react with the surrounding air because they tend to absorb moisture from the atmosphere (Feng et al., 2023). This finding suggests that the snail shell, which is utilized as a precursor to calcium in the creation of hydroxyapatite (HAp), may find application in other processes. Figure 1 shows the functionality clusters that were found within the FTIR spectrum.

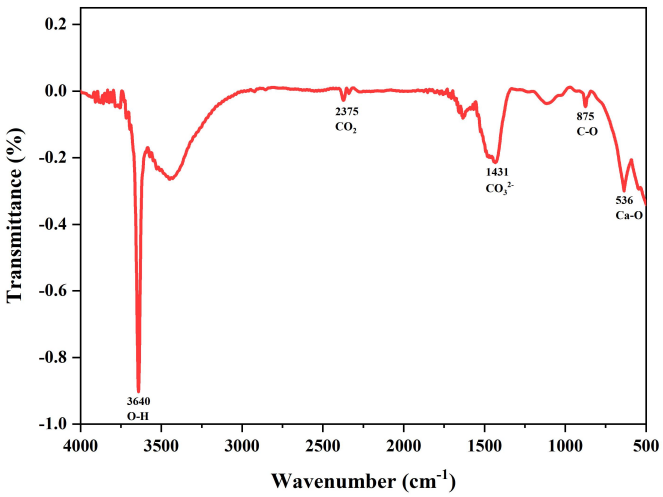

Figure 1. FTIR Spectrum of CaO

To confirm the crystalline phase of the resultant CaO, the calcined CaO precursors were additionally submitted to XRD (X-ray diffraction) examination (Figure 2). The XRD analysis results showed that the diffraction pattern of CaO changed to display $Ca(OH)_2$, as demonstrated by the peaks that matched in the sample and the reference. $Ca(OH)_2$ crystalline phase was identified by verifying XRD peaks using JCPDS data No. 01-072-0156. The results at an angle of 2θ 33.9884 with a factual intensity of 100%; 47.0180 with a factual intensity of 40.10%; 50.7369 with a factual intensity of 25.3%; and 54.2133 with a factual intensity of 13.7% all fit the high-intensity XRD pattern of $Ca(OH)_2$. A crystal size of 14.087 nm with a crystallinity of 69.8740% was also obtained based on the findings of the XRD Difractogram $Ca(OH)_2$.

3.2 HAp-Fe_3O_4 Composite

Researchers used a coprecipitation approach to synthesize HAp-Fe_3O_4 composites due to its ease of use and the tendency of iron salts to bind to hydroxyapatite in solution (Matei et al., 2017). A molar ratio 1:1 was used in the HAp and Fe_3O_4

Table 1. Percentage Reduction in $CaCO_3$ Powder Weight before and after Calcination

Calcination Temperature (°C)	$CaCO_3$ Weight After Calcination (g)	CaO Weight After Calcination (g)	CaO weight after 7 days (g)	Weight Loss (g)	Weight Reduction (g)
1000	19.3320	10.5484	14.1142	8.7836	45.4355

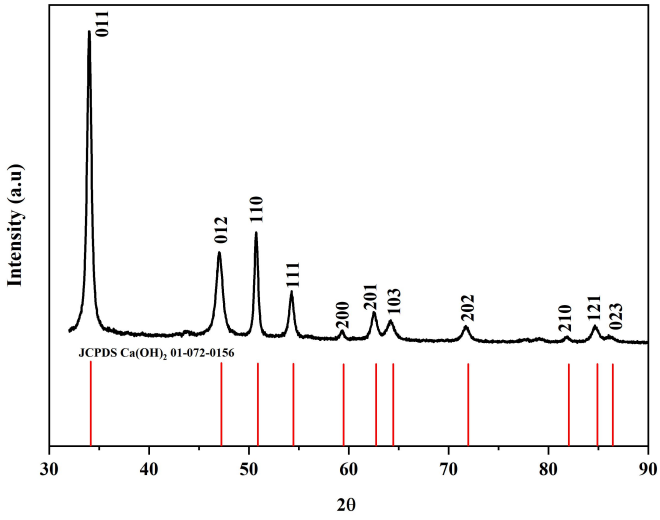

Figure 2. XRD Patterns of CaO

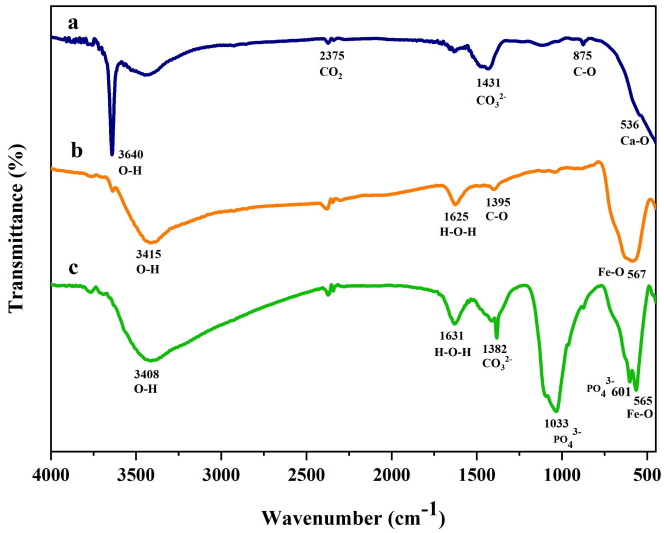

Figure 3. FTIR Spectrum of A) CaO B) Fe_3O_4 C) HAp-Fe_3O_4 composite

composite method to ensure significant end products (Mushtaq et al., 2021). The iron solution, containing $FeCl_3$ as the Fe^{3+} source and $FeCl_2$ as the Fe^{2+} source, was combined with CaO from field snail shells and $(NH_4)_2HPO_4$ as the hydroxyapatite source to prepare the composites. The researchers chose the Fe source for utilization due to its high solubility in water.

Moreover, the $FeCl_3$ and $FeCl_2$ solutions show robust electrolyte characteristics that facilitate the solutes' breakdown into ions and the appropriate production of Fe_3O_4. During processing, Researchers add NH_4OH solution to the combination as a precursor in the Hydroxyapatite (HAp) composite with an iron solution. This process lasts for two hours at a temperature of 90 °C while continuously stirring. Adding the NH_4OH solution to the mixture containing the iron solution and HAp causes a brownish-black precipitate, indicating the successful creation of the hydroxyapatite-magnetite composite.

Temperature is a critical component that affects the formation process during the synthesis and manufacture of composites. Applying a temperature of 90 °C can consequently create dull remains, powers the chemical responses that happen amid the amalgamation of magnetite. Raising the temperature produces sufficient active vitality to induce past the actuation vitality resistance and animates the response rate (Biedrzycka et al., 2021). The nearness of dark particles connected with attractive areas subjectively depicts the HAp-Fe_3O_4 composite. This dark composite store is waterproof and will float toward it when near a gorgeous field. The dark acceleration delivered in this examination contained magnetite (Fe_3O_4). Afterward, rinsing the composite deposits with an aqueous solution eliminates contaminants in the form of Cl^- ions. Moreover, the rinsing procedure helps to align the pH with the aqueous, which has a pH of roughly 7. The composite residues are dried in an oven warmed to 110 °C for two hours after rinsing.

3.3 IR Spectrum Composite of HAp-Fe_3O_4

The hydroxyapatite and magnetite composites were analyzed to get data on the composite structure through a few characterizations. The FTIR range can survey the victory of segregating hydroxyapatite from *Bellamya javanica* shells and synthesizing HAp-Fe_3O_4 composites in this ponder. This method is essential for detecting the functional groups in the specimen. Figure 3 illustrates the FTIR analysis of magnetite, hydroxyapatite obtained from *Bellamya javanica* shells, and HAp-Fe_3O_4 composites. According to the findings of the FTIR analysis of the HAp-Fe_3O_4 composites, the presence of O−H absorption bands from the hydroxyl (OH^-) group at a peak of 3410 cm^{-1}, the phosphate (PO_4^{3-}) group indicated by the presence of P−O vibration at peaks of 1032 cm^{-1} and 601 cm^{-1}, and the CO_3^{2-} group at a peak of 1382 cm^{-1} demonstrated the hydroxyapatite content.

The solid retention of Gracious and PO_4^{3-} bunches infers the creation of hydroxyapatite gems. Be that as it may, the nearness of CO_3^{2-} bunches proposes that the calcium source

confined from *Bellamya javanica* shells contains $CaCO_3$, which needs to change to CaO. A hydrated O−H bunch illustrates the victory of composite amalgamation, with H−O−H vibration recognized at a wave number of 1631 cm^{-1} for HAp-Fe_3O_4 composites. These hydrated O-H groups are formed during the composite manufacturing process and are present in the HAp-Fe_3O_4 composite due to the involvement of water (Vahdat et al., 2019). The hydrated O−H groups further indicate the success of the composite synthesis, with H−O−H vibrations detected at a wave number of 1631 cm^{-1} for the HAp-Fe_3O_4 composite. These hydrated O−H groups are formed during the composite manufacturing process and are present in the HAp-Fe_3O_4 composite due to the involvement of water (Vahdat et al., 2019).

Furthermore, the appearance of the Fe−O functional group at peaks 567 cm^{-1} and 565 cm^{-1} indicates the presence of magnetite concentration. The appearance of the H−O−H functional group at peak 1625 cm^{-1} indicates O−H hydration to the Fe_3O_4 surface. The number of waves in the magnetite functional group indicates a shift in the HAp-Fe_3O_4 composite. These findings indicate that the FTIR spectrum indicates the presence of compositional interactions between magnetite and hydroxyapatite (Radon et al., 2017).

3.4 XRD Patterns of Hap-Fe_3O_4 Composite

X-ray diffraction (XRD) analysis identified and confirmed the crystal structure of the specimen by comparing its composition with the 2θ value reported in the literature. JCPDS 00-019-0629 is the Fe_3O_4 phase used in this study, while the standard literature is the hydroxyapatite phase. JCPDS 04-00-09-32. This XRD investigation involved HAp-Fe_3O_4 composites. Figure 4 shows the diffractograms from the XRD study.

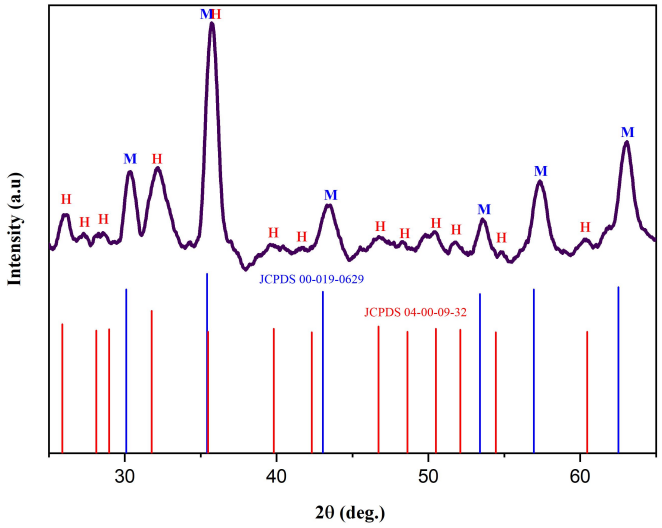

Figure 4. XRD Patterns of HAp-Fe_3O_4 composite H) HAp M) Magnetite

The analysis identified the results of the diffractogram by matching the data obtained at the diffraction peaks at the angle of 2θ. The peak of diffraction formed with the maximum intensity representing hydroxyapatite is at an angle of 2θ = 31.971°; 25.937°; and 46.741° corresponding to the Miller index at an angle of 2θ = 31.774°; 25.879°; and 46.713°. These findings corroborate Sneha et al. (2016), who observed the development of hydroxyapatite in the diffractogram at an angle of 2θ = 31.76°. The results demonstrate that hydroxyapatite does indeed form in composite materials. Meanwhile, the diffraction pattern formed for the maximum intensity representing Fe_3O_4 is at an angle of 2θ = 35.755°; 62.993°; and 30.290° corresponding to the Miller index at an angle of 2θ = 35.423°; 62.516°; and 30.095°. The synthesis produced a HAp-Fe_3O_4 composite.

This research analyzed the compound abundance with a diffraction angle of 2θ and crystal structure, as well as the dimensions of crystals and the proportion of crystalline content in composite specimens using XRD evaluation. The HAp-Fe_3O_4 composite's crystal sizes and crystalline content percentage were measured at 7.63125 nm and 84.7879%, respectively. Based on these results, we can conclude that the HAp-Fe_3O_4 composite has a small crystal size and comparatively high crystallinity %. Vesali-Naseh et al. (2021) discovered that the HAp-Fe_3O_4 composite had a crystal size of 14.1 nm, as measured in this study. Lubis et al. (2020) noted that a nanomaterial's hardness and tensile strength often improve with increasing surface area as its size decreases. The more important surface zones of the HAp-Fe_3O_4 composites increase their adsorption capacity and make them stronger adsorbents. According to Fatima et al. (2024), a better proportion of regular structured gemstones in the test is associated with subsequent crystallinity levels, which results in a higher basic normality level in the HAp-Fe_3O_4 composites used in this study.

3.5 SEM-EDX Morphology of HAp-Fe_3O_4 Composite

The study utilized SEM-EDX to portray the HAp-Fe_3O_4 composite test. SEM assessed the test's morphology and particle size, while EDX determined the elemental composition and validated the composite's Pb content and Ca/P ratio before and after the material was adsorbed (Akhlaghinia et al., 2019). The image was taken with a voltage of 15 kV, particle sizes of 20 and 50 μm, and a magnification of 1000×. Images of the surface morphology of the HAp-Fe_3O_4 composites both before and following adsorption are displayed in Figure 5.

The pre-adsorption composite SEM image of HAp-Fe_3O_4 showed a uniform shape. The HAp-Fe_3O_4 composite, which was synthesized before adsorption, appears to be made up of granular or solid-shaped particles, with the Fe_3O_4 morphology shaped like a tetragonal cubic with a long rod-like shape surrounded by small hydroxyapatite grains, according to Figure 5a surface morphology. This hydroxyapatite has irregular grains and a porous structure, typically having an agglomeration or clump-like appearance (Abidin et al., 2020). The composite, composed of tiny particles and pores, is an adsorbent. When the particles come together, they form solids, but

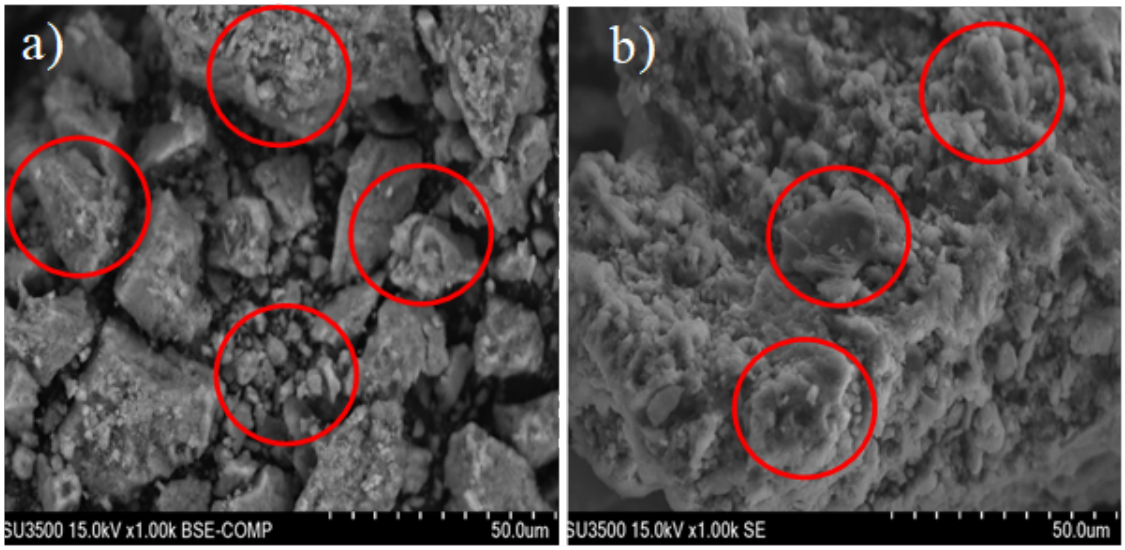

Figure 5. SEM Morphology Composite HAp-Fe_3O_4 a) before b) after Adsorption

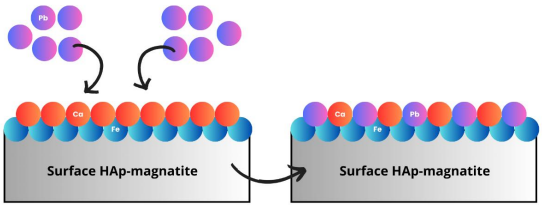

Figure 6. Illustration of Multilayer Exchange of Ca^{2+} and Pb^{2+} Ion Cations

their morphology remains apparent. ImageJ and the Root software confirmed the approximate measurement of 10.984 μm for the composite's molecules. Smaller molecules have more amazing surface ranges, which enable strong metal adsorption.

The HAp-Fe_3O_4 composite SEM image results after adsorption showed a non-uniform morphology. The surface morphology in Figure 5b shows that the HAp-Fe_3O_4 composite synthesized after adsorption appears to be composed of granular/shape agglomerates. The particles combine to form agglomerated solids whose morphology is less obvious. The denser morphological changes and tighter particle sizes in the composites after adsorption suggest that the composite surfaces containing hydroxy groups on the hydroxyapatite surfaces allow for solid interactions between heavy metal ions and hydroxyapatite (Akhlaghinia et al., 2019). According to this research, hydroxyapatite is a very effective way to remove heavy metal ions from solutions. Metal adsorption onto Hydroxyapatite (HAp) can be ascribed to different components, including the substitution of metal particles with calcium particles (Ca^{2+}), the arrangement of metal-phosphate complexes, and chemical intuitive with hydroxyl bunches on the HAp surface (Yang et al., 2021). Moreover, ionic exchange with Pb ions with a 2+ charge

Table 2. Elemental Content in HAp-Fe_3O_4 Composite Samples from EDX

Sample	Content	Weight (%)	Ca/P
HAp-Fe_3O_4 Before Adsorption	Ca	15.52	1.53
	P	7.86	
	Fe	45.59	
	O	31.03	
HAp-Fe_3O_4 After Adsorption	Ca	9.74	1.25
	P	6.04	
	Fe	30.69	
	O	49.02	
	Pb	4.51	

can increase hydroxyapatite's adsorption capability.

Since calcium ions in hydroxyapatite have a 2+ charge, they can exchange with other ions of similar charge, especially 2+. Particles in HAp-Fe_3O_4 composites usually have tiny diameters. By entering the HAp network, Fe_3O_4 can affect the development and morphology of particles during the amalgamation process. Furthermore, the expansion of Fe3O4 may affect the system's molecule estimate dispersion. Littler particles are delivered in general due to the interaction between Fe_3O_4 and HAp, which can improve uniform molecule scattering. After adsorption, the components Pb and Ca, P, Fe, and O were present in the sample, according to the EDX results in Table 2 Oxygen (O) 31.03%, Phosphorus (P) 7.86%, Calcium (Ca) 15.52%, and Iron (Fe) 45.59% for composites before adsorption and Oxygen (O) 49.02%, Phosphorus (P) 6.04%, Calcium (Ca) 9.74%, Iron (Fe) 30.69%, and Lead (Pb) 4.51% for composites after adsorption.

The results of the EDX examination found the elemental

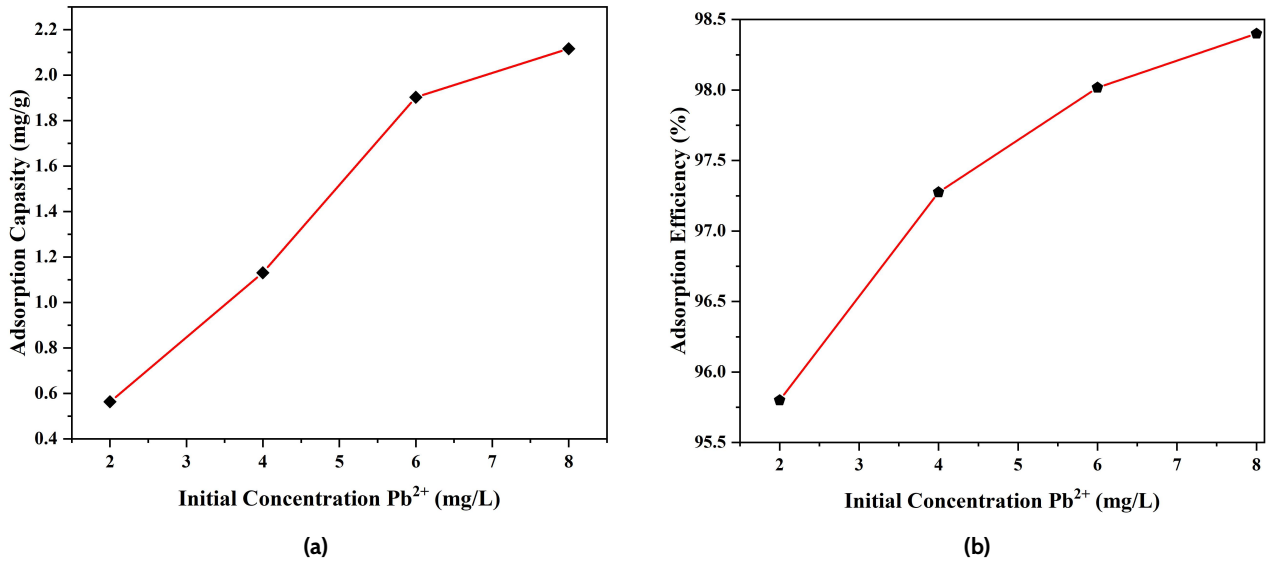

Figure 7. a) Adsorption Capacity Curve b) Efficiency Curve of HAp-Fe_3O_4 Composite Against Pb Metal Ions

composition of the magnetite and hydroxyapatite materials. The EDX examination revealed that the composites' Ca/P proportion was 1.25 after adsorption and 1.53 before adsorption. The distinction in stoichiometric moles between the phosphorus (P) and calcium (Ca) atoms within the hydroxyapatite crystal lattice is made clear by this comparison of Ca/P ratios. The study's Ca/P ratio, which shows the formation of hydroxyapatite compound, is reasonably equivalent to the 1.67 standard Ca/P ratio (Yang et al., 2021).

Table 2 indicates that both before and after adsorption, the composite Ca/P ratio falls. Due to Pb^{2+} having the same charge as Ca^{2+}, Pb^{2+} ions can replace Ca^{2+} ions in the hydroxyapatite structure when the composite absorbs Pb metal. Furthermore, Pb^{2+} ions can substitute Ca^{2+} ions in the crystal lattice or molecular structure without severely distorting it due to the comparable ion sizes of Ca^{2+} (114 pm) and Pb^{2+} (133 pm) (Figure 6). The addition of Pb metal mass increases the total mass of the composite. The Ca/P concentration will drop relative to the increase in mass if insufficient Ca or P is added to make up for it. The interaction of Pb metal with the composites can change the structure, composition, and even the redistribution of the constituent parts of HAp-Fe_3O_4 composites. Calcium (Ca) and phosphorus (P) levels in the composite material may decrease. The interaction represented by reaction Equation 7 involves the exchange of Ca^{2+} ions at the Hydroxyapatite (HAp) surface with Pb^{2+} ions.

$$Ca_{10}(PO_4)_6(OH)_2 + X Pb^{2+} \rightarrow Ca_{10-x}Pb_x(PO_4)_6(OH)_2 + X Ca^{2+} \quad (7)$$

3.6 Adsorption of HAp-Fe_3O_4 Composite

Adsorption includes HAp-Fe_3O_4 composite adsorbents to a lead ion-containing arrangement (II). Once the adsorption process wraps up, the liquid and its adsorbent are isolated. Furthermore, AAS measured the Pb(II) metal particles absorbed by the composite adsorbent. Agreeing with the procedure portrayed within the think about by Vahdat et al. (2019), the exploratory settings included an adsorbent mass of 0.03 grams at pH 6, an arrangement volume of 10 mL, and a concentration extend of 2-8 ppm (in increases of 2). Adsorption happens in a bunch framework with a vortex gadget, blending the adsorbent and adsorbate for 40 minutes at 200 rpm at room temperature (25 °C). Figure 7 shows the lead(II) metal particle adsorption measurements on the HAp-Fe_3O_4 composite.

Figure 7a shows lead(II) metal particle concentrations between 2 and 8 parts per million, appearing in the adsorption capacity. The concentration of lead(II) metal particles in a fluid arrangement improves an adsorbent's capacity to adsorb lead(II) metal. Mohammadi Aghdam et al. (2018) claim that an increment in the number of purge pores within the composite adsorbents is the reason. Figure 7a illustrates the peak adsorption capacity of the HAp-Fe_3O_4 composite adsorbent at two ppm. This capability increases up to an eight-ppm concentration. These results demonstrate how successfully lead(II) metal ions are captured by the adsorbent at high concentrations. A plausible rationale for the consistent increase in adsorption at elevated doses could be a reduction in it.

The following result is based on the adsorption efficiency shown in Figure 7b, where an increase in solution concentration from 2 ppm to 8 ppm causes the adsorption efficiency to improve from 95.80% to 98.40%. The findings demonstrated that the HAp-Fe_3O_4 composite was effective at capturing lead(II) ions in solution since it enhanced the adsorption effectiveness of the metal ions as the solution's concentration increased (Shi et al., 2021). Lead ion adsorption efficiency can be increased by up to 8 ppm using HAp-Fe_3O_4 composites. Lead ion ad-

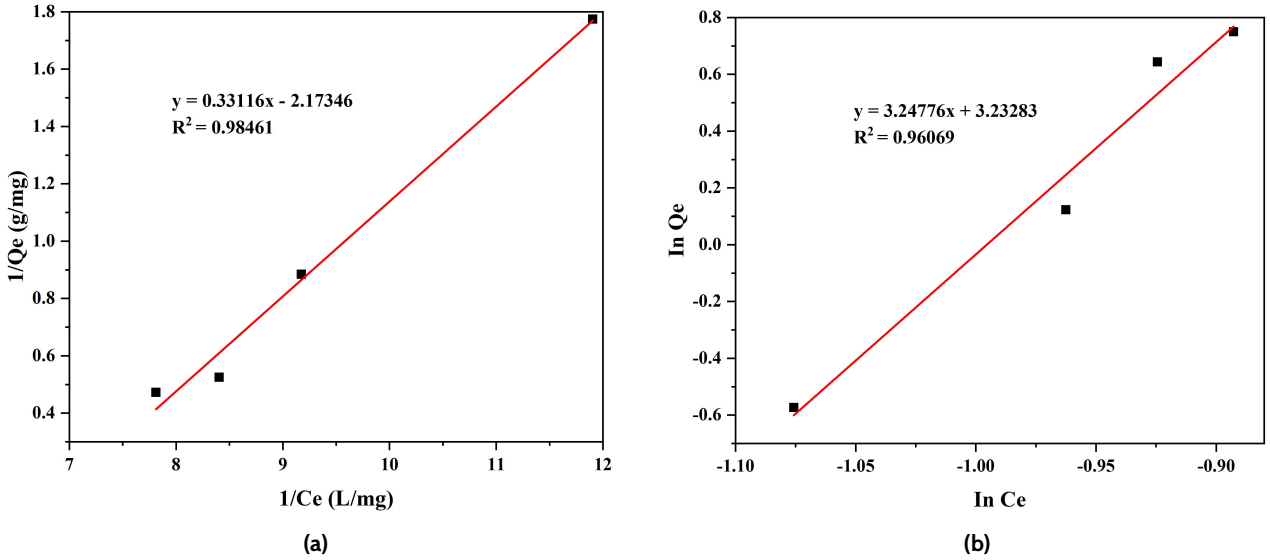

Figure 8. Adsorption Isothermal Curve a) Langmuir b) Freundlich

sorption efficiency can be increased by up to 8 ppm using HAp-Fe_3O_4 composites. The interconnectivity of adsorbent pores or a drop in the concentration of metal ions in an aqueous solution for adsorption in composite pores may be responsible for the adsorption efficiency fixed at large adsorbent concentrations. Thus, with concentrations between 2 and 8 parts per million, eight parts per million implies the optimal lead ion removal threshold.

The results of adsorption efficiency, when compared to previous studies that used various sources of hydroxyapatite, showed better results with a greater efficiency percentage. The high adsorption efficiency indicates that the adsorbent can attract and retain adsorbates from the solution. The HAp-Fe_3O_4 composite adsorbent derived from tuft shells has many active sites or a large surface area for interaction with adsorbates. Therefore, using this tutu shell-based HAp-Fe_3O_4 composite as an adsorbent for handling heavy metal waste, especially lead (Pb), is feasible. The adsorption efficiency results from previous studies and this study are presented in Table 3.

Table 3. Comparison of % Adsorption Efficiency of HAp-Fe_3O_4 Composites from Various Sources Hydroxyapatite Against Pb Metal Ions

HAp Source	Efficiency (%)	Reference
$Ca(NO)_3.4H_2O$	89.00	Hui et al. (2021)
Chicken Bones	95.74	Vahdat et al. (2019)
Beef Bones	74.20	Salsabila et al. (2023)
Bellamya javanica Shell	98.40	This Research

3.7 Adsorption Isoterm

An isothermal show looks at how the fluid and strong stages harmonize. Adsorption isotherms encourage a distant, much better, more robust, and improved understanding of the adsorption component between the adsorbent surface and the adsorbate arrangement. Since ionic or covalent associations are shaped amid chemical responses, homogeneous adsorbent surfaces ordinarily retain adsorbate materials at their best layers. The concept of monolayer adsorption is explained via the Langmuir isotherm (Al-Ghouti and Da'ana, 2020). The Langmuir isothermal model has shown utility for homogeneous single-layer adsorption processes in several situations (Ng et al., 2017). Conversely, the physical adsorption process takes place on what is known as Freundlich isotherms, which are heterogeneous adsorbent surfaces (Wang and Guo, 2020). Both Freundlich and Langmuir isotherms are present in most HAp-Fe_3O_4 composites; however, one is usually more prominent.

The 40-minute Pb(II) ion adsorption experimental data were fitted to isothermal linear equations using the HAp-Fe_3O_4 composite to determine the intrinsic parameters of the Freundlich and Langmuir isotherms. Figures 8a and 8b present the results graphically. The values of K_L and Q_m for the Langmuir isotherm are shown in Table 4 and were derived from the slope of the linearity plot of $1/C_e$ vs $1/Q_e$ in Figure 8a. The values of K_F and $1/n$ from the linear plot of log Q_e against log C_e in Figure 8b, which depicts the Freundlich isotherm, are also listed in Table 4. The linearity plot shown in Figure 8 indicates that the Langmuir equation yields superior outcomes to the Freundlich isotherm.

The results of the adsorption equilibrium analysis indicate that the Freundlich plot has a determination coefficient of R^2 = 0.96069, while the Langmuir plot suggests a significant connec-

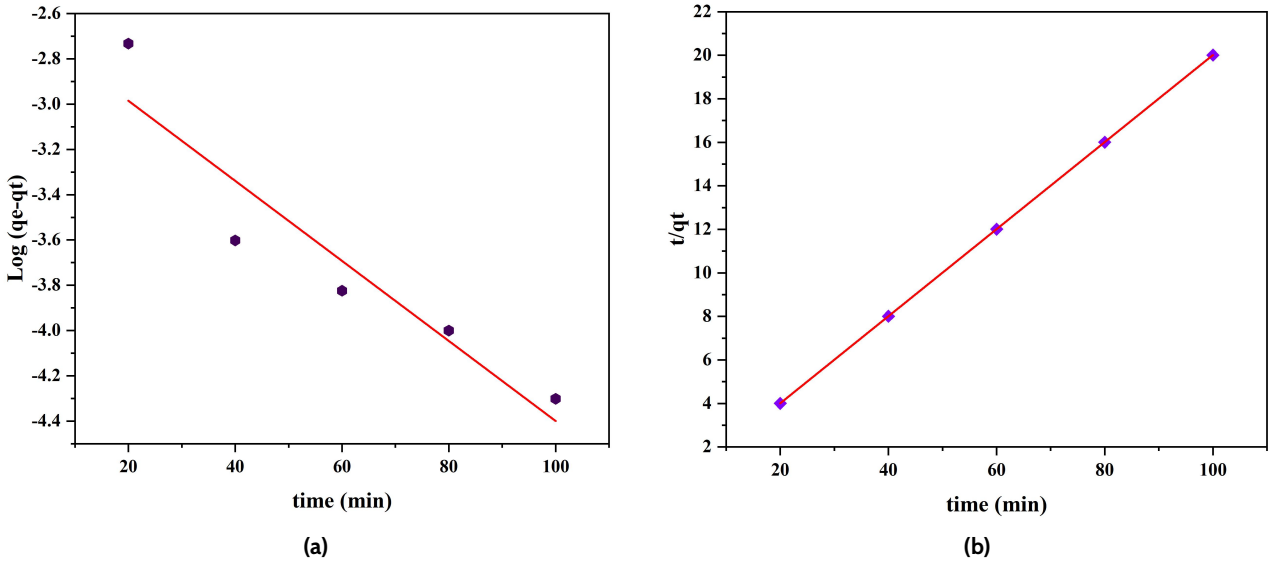

Figure 9. Kinetic Curve a) Pseudo-First-Order b) Pseudo-Second-Order

Table 4. Isothermal Constants of HAp-Fe_3O_4 Composite Adsorption on Pb(II) Ions

Langmuir Isotherm				Freundlich Isotherm			
Q_m	K_L	R_L	R^2	n	$1/n$	K_F	R^2
3.0197	-0.1524	-1.9097	0.9846	3.2478	0.3097	25.3513	0.9607

Table 5. The Kinetic Parameters for the Pb Ion Adsorption Process Using HAp-Fe_3O_4 Adsorbent

Adsorbent	Q_e exp (mg/g)	Models		
HAp-Fe_3O_4	4.9977	PFO	Q_e calc (mg/g)	0.0023
			K_1 (min^{-1})	0.0407
			R^2	0.8851
		PSO	Qe calc (mg/g)	4.9980
			K_2 (g/mg.min)	29.7480
			R^2	1

tion with the experimental data, with R^2 = 0.98461. However, a negative K_L value was noted for the Langmuir isotherm, indicating that the interaction could not be clarified when the HAp-Fe_3O_4 adsorbent adsorbed Pb(II) ions. The Freundlich isotherm is a more appropriate choice when modeling the equilibrium of Pb(II) ion adsorption using HAp-Fe_3O_4 adsorbents.

The maximum adsorption capacity indicates the highest number of molecules the surface can adsorb. In contrast, the Langmuir constant (K_L) parameter value characterizes the intensity of contact between the adsorbent molecules and the solid surface (Ng et al., 2017). Meanwhile, the adsorption intensity and capacity, or non-linearity, regarding the adsorbate at low concentrations are indicated by the Freundlich isotherm model's n and K_F parameter values (Vahdat et al., 2019).

Therefore, the HAp-Fe_3O_4 composite surface has heterogeneous active sites for the adsorption of Pb(II) ions, which allows multilayer adsorption. Further evidence that the adsorption mechanism is a sequential process on the adsorbent surface comes from using the Freundlich isotherm in this study (Abidin et al., 2020). The Freundlich isotherm numbers between 1 and 10 are considered favorable for adsorption, according to Atkins et al. (2018). In addition, the adsorbent is in a good position when the 1/n ratio is less than one. This number indicates a strong adsorbent-adsorbate contact that keeps the adsorbate from separating from the adsorbent surface. The current study shows that the HAp-Fe_3O_4 composite is very effective as an adsorbent in the adsorption process of Pb(II) ions, as evidenced by the n value of 3.248 and the $1/n$ value of 0.308. This contact between the adsorbent and the adsorbate ensures an efficient adsorption process.

The discoveries outlined in Table 4 demonstrate that the K_F esteem, the most reduced relative adsorption capacity of adsorbents inferred from this examination, is 25.351 L/g. This perception underscores the power and viability of adsorption.

Table 6. The Thermodynamic Parameters for the Pb Ion Adsorption Process Using HAp-Fe_3O_4 Adsorbent

Adsorbent	T (K)	ΔG° (KJ/mol)	ΔH° (KJ/mol)	ΔS° (KJ/mol)
HAp-Fe_3O_4	298.15	-1.2010	3.3084	4.0394
	303.15	-1.2212		
	313.15	-1.2616		
	333.15	-1.3424		

In essence, at equilibrium, there is a tendency for many chemicals to be adsorbent per unit mass of adsorbents. The notably favorable values of $1/n$ and K_F demonstrate the exceptional efficiency of the HAp-Fe_3O_4 composite adsorbent, suggesting its viability as an eco-friendly option for adsorbing Pb(II) ions.

3.8 Kinetic and Thermodynamic Study

Adsorption kinetics determine the controlling mechanisms of adsorption processes, such as surface adsorption, chemical reactions, and penetration mechanisms. Several models have been used in the past to study adsorption kinetics. This study used the first-order and second-order kinetic models to investigate the adsorption kinetic behavior of Pb metal ions using HAp-Fe_3O_4 composite. Pseudo-first-order (PFO) and pseudo-second-order (PSO) models were used to analyze the adsorption kinetics

The experimental adsorption data were fitted to the kinetics and isotherm models to gain useful knowledge about the adsorption process and behavior. The resulting lines of both kinetic models are shown in Figure 9, and the corresponding variables are specified in Table 5. Based on the kinetic results obtained, the PSO model provides a better fit to the experimental data, as indicated by the higher R^2 value compared to the PFO model. The Q_e values calculated using the PSO model are also closer to the experimental values. PSO indicates a chemical process and assumes that the adsorption rate depends on the square of the amount of adsorbate on the surface, and Pb^{2+} ions chemically bind to the active sites of the HAp-Fe_3O_4 composite. This indicates a strong interaction between the metal ions and the composite surface. This process may involve electron transfer or covalent bond formation between Pb^{2+} and functional groups on the composite material surface.

The experimental adsorption data were fitted to the kinetics and isotherm models to gain useful knowledge about the adsorption process in this study to evaluate the process behavior, we investigated thermodynamic parameters such as enthalpy (ΔH°), entropy (ΔS°), and Gibbs free energy (ΔG°). The values of ΔH° and ΔS° were determined from the slope and intercept of the InKD vs 1/T curve (Figure 10), and their values are shown in Table 6.

The Gibbs free energy calculated for the lead ion adsorbent is negative, indicating that it is thermodynamically optimal and spontaneous. In addition, the ΔH° value is positive, indicating that the interaction between the adsorbent and lead ions is endothermic. It also indicates that the adsorption process of lead metal using the adsorbent is physical because ΔH° is less than 40 KJ/mol. The sum of ΔS° is negative for the lead ion adsorption process, indicating reduced random collisions of lead ions in the solid (adsorbent) and aqueous solution during adsorption.

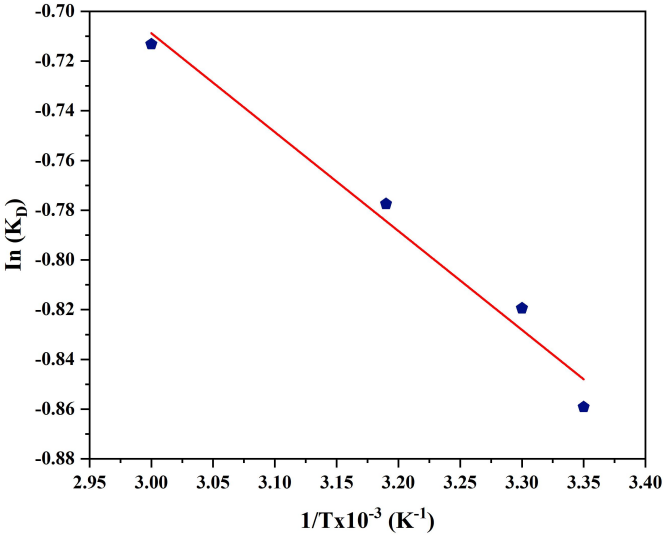

Figure 10. The plot of In KD versus 1/T for adsorption of Pb(II) by the HAp-Fe_3O_4

4. CONCLUSIONS

HAp-Fe_3O_4 composites can be synthesized from *Bellamya javanica* snail shells and magnetite as base materials. The presence of hydroxyapatite and magnetite was confirmed through FTIR, XRD, and SEM-EDX characterization, which detected calcium, phosphate, iron, and oxygen in the composite samples. The abundant calcium content is the primary precursor in HAp synthesis, while the plentiful iron content is the primary magnetite precursor. The composite sample's phrase, crystal size, and Ca/P ratio were also determined. The adsorption capacity and efficiency of HAp-Fe_3O_4 composites in absorbing Pb(II) ions show that as the solution concentration increases, both the adsorption capacity and efficiency increase. Isothermal adsorption of HAp-Fe_3O_4 composite adsorbents follows the Freundlich isothermal equation, indicating a multilayer adsorption process. This adsorption process is highly profitable because the adsorbate adheres firmly to the adsorbent surface, ensuring optimal adsorption performance. A kinetic study of the process found that pseudo-second-order kinetic

models have the potential to describe the kinetic behavior of the adsorption process. Thermodynamic parameters such as enthalpy, entropy, and Gibbs free energy were also studied, and found that the adsorption of lead ions using the adsorbent is endothermal and spontaneous.

5. ACKNOWLEDGMENT

The authors acknowledge to the Ministry of Education, Culture, Research, and Technology, Directorate of Research and Innovation IPB University, Department of Chemistry IPB University, the facilities, scientific and technical support from Advanced Characterization Physics Laboratories Serpong, National Research and Innovation Agency.

REFERENCES

Abidin, N. H. Z., N. S. Sambudi, and N. A. Kamal (2020). Composite of Hydroxyapatite-Fe_3O_4 for the Adsorption of Methylene Blue. *ASEAN Journal of Chemical Engineering*, **20**(2); 140–153

Akhlaghinia, B., P. Sanati, A. Mohammadinezhad, and Z. Zarei (2019). The Magnetic Nanostructured Natural Hydroxyapatite (HAP/Fe_3O_4 NPs): An Efficient, Green and Recyclable Nanocatalyst for the Synthesis of Biscoumarin Derivatives under Solvent-Free Conditions. *Research on Chemical Intermediates*, **45**(5); 3215–3235

Al-Ghouti, M. A. and D. A. Da'ana (2020). Guidelines for the Use and Interpretation of Adsorption Isotherm Models: A Review. *Journal of Hazardous Materials*, **3**(1); 1–100

Atkins, P., J. De Paula, and J. Keeler (2018). *Physical Chemistry*. Oxford University Press, 11th edition

Biedrzycka, A., E. Skwarek, and U. M. Hanna (2021). Hydroxyapatite with Magnetic Core: Synthesis Methods, Properties, Adsorption and Medical Applications. *Advances in Colloid and Interface Science*, **29**(1); 1–21

Diningsih, C. and L. Rohmawati (2022). Synthesis of Calcium Carbonate ($CaCO_3$) from Eggshell by Calcination Method. *Indonesian Physical Review*, **5**(3); 208–215

El-Dib, F. I., D. E. Mohamed, O. A. A. El-Shamy, and M. R. Mishrif (2020). Study the Adsorption Properties of Magnetite Nanoparticles in the Presence of Different Synthesized Surfactants for Heavy Metal Ions Removal. *Egyptian Journal of Petroleum*, **29**(1); 1–7

Fatima, E., I. Arooj, M. Javeed, and J. Yin (2024). Green Synthesis, Characterization and Applications of *Phyllanthus emblica* Fruit Extract Mediated Chromium Oxide Nanoparticles. *Discover Nano*, **19**(1); 68

Feng, Y., X. Li, H. Wu, C. Li, M. Zhang, and H. Yang (2023). Critical Review of $Ca(OH)_2$/CaO Thermochemical Energy Storage Materials. *Energies*, **16**(1); 13932–13936

Hafez, M., M. Kassab, and S. Taha (2021). Calcination Process and Kinetic Carbonation Effect on the Hydrated and Anhydrate Phases of the OPC Matrix at Early Age of Hydration. *HBRC Journal*, **17**(1); 389–406

Hui, K. C., N. A. Kamal, N. S. Sambudi, and M. R. Bilad (2021). Magnetic Hydroxyapatite for Batch Adsorption of Heavy Metals. In *E3S Web of Conferences*, volume 28. pages 3–8

Lubis, R. A. F., H. I. Nasution, and M. Zubir (2020). Production of Activated Carbon from Natural Sources for Water Purification. *Indonesian Journal of Chemical Science and Technology (IJCST)*, **3**(2); 67–73

Martinez, J., J. L. Wardini, X. Zheng, L. Moghimi, J. Rakowsky, J. Means, H. Guo, I. Kuzmenko, J. Ilavsky, F. Zhang, P. P. Dholabhai, L. Dresselhaus-Marais, and W. J. Bowman (2024). Precision Calcination Mechanism of $CaCO_3$ to High-Porosity Nanoscale CaO CO_2 Sorbent Revealed by Direct In Situ Observations. *Advanced Materials Interfaces*, **11**(14); 1–9

Matei, E., A. Predescu, C. Dragan, C. Pantilimon, and C. Predescu (2017). Characterization of Magnetic Nanoiron Oxides for the Removal of Metal Ions from Aqueous Solution. *Analytical Letters*, **50**(17); 2822–2838

Mielke, H. W., C. R. Gonzales, E. T. Powell, and S. P. Egendorf (2022). Lead in Air, Soil, and Blood: Pb Poisoning in a Changing World. *International Journal of Environmental Research and Public Health*, **19**(15); 1–30

Mohamed, F., M. Shaban, G. Aljohani, and A. M. Ahmed (2021). Synthesis of Novel Eco-Friendly CaO/C Photocatalyst from Coffee and Eggshell Wastes for Dye Degradation. *Journal of Materials Research and Technology*, **14**; 3140–3149

Mohammadi Aghdam, S., B. Valinezhad Saghezi, Y. Mortazavi, and S. M. Qhoreishi (2018). Modified Fe_3O_4/HAP Magnetically Nanoparticles as the Carrier for Ibuprofen: Adsorption and Release Study. *Drug Research*, **69**(2); 93–99

Murmu, R., S. M. George, P. Yuvarani, P. Bhatnagar, K. Amudha, C. Engineering, G. Noida, and T. Nadu (2024). Sustainable Solutions for Heavy Metal Contamination: Characterization and Regeneration of Water Hyacinth Biosorbent in Wastewater Treatment. *26(X)*; 1–8

Mushtaq, A., R. Zhao, D. Luo, E. Dempsey, X. Wang, M. Z. Iqbal, and X. Kong (2021). Magnetic Hydroxyapatite Nanocomposites: The Advances from Synthesis to Biomedical Applications. *Materials and Design*, **19**(7); 1–54

Ng, K. C., M. Burhan, M. W. Shahzad, and A. B. Ismail (2017). A Universal Isotherm Model to Capture Adsorption Uptake and Energy Distribution of Porous Heterogeneous Surface. *Scientific Reports*, **7**(1); 1–11

Ngouoko, J. J. K., K. Y. Tajeu, C. G. Fotsop, A. K. Tamo, G. Doungmo, R. C. T. Temgoua, T. Kamgaing, and I. K. Tonle (2022). Calcium Carbonate Originating from Snail Shells for Synthesis of Hydroxyapatite/L-Lysine Composite: Characterization and Application to the Electroanalysis of Toluidine Blue. *Crystals*, **12**(9); 1189

Noh, Y. K., A. Dos Santos Da Costa, Y. S. Park, P. Du, I. H. Kim, and K. Park (2019). Fabrication of Bacterial Cellulose-Collagen Composite Scaffolds and Their Osteogenic Effect on Human Mesenchymal Stem Cells. *Carbohydrate Polymers*, **219**; 210–218

Radon, A., A. Drygala, L. Hawelek, and D. Lukowiec (2017).

Structure and Optical Properties of Fe_3O_4 Nanoparticles Synthesized by Co-Precipitation Method with Different Organic Modifiers. *Materials Characterization*, **131**; 148–156

Saikumari, N., S. M. Dev, and S. A. Dev (2021). Effect of Calcination Temperature on the Properties and Applications of Bio Extract Mediated Titania Nano Particles. *Scientific Reports*, **11**(1); 1–17

Salsabila, N., V. Amalia, and R. Fitriyani (2023). Synthesis and Characterization of HAp/Fe_3O_4 Composite from Cow Bone as Lead (II) Metal Ion Adsorbent. *Journal Chemistry*, **1**(1); 49–59

Santucci, R. J. and J. R. Scully (2020). The Pervasive Threat of Lead (Pb) in Drinking Water: Unmasking and Pursuing Scientific Factors That Govern Lead Release. *Proceedings of the National Academy of Sciences of the United States of America*, **117**(38); 23211–23218

Shi, W., M. Xia, F. Wang, L. Dong, and S. Zhu (2021). Efficient Absorption Properties of Surface Grafted HEDP-HAP Composites for Pb^{2+} and Cu^{2+}: Experimental Study and Visualization Study of Interaction Based on Becke Surface Analysis and Independent Gradient Model. *Journal of Hazardous Materials*, **401**; 1–12

Sneha, M., N. Meenakshi Sundaram, and A. Kandaswamy (2016). Synthesis and Characterization of Magnetite/Hydroxyapatite Tubes Using Natural Template for Biomedical Applications. *Bulletin of Materials Science*, **39**(2); 509–517

Vahdat, A., B. Ghasemi, and M. Yousefpour (2019). Synthesis of Hydroxyapatite and Hydroxyapatite/Fe_3O_4 Nanocomposite for Removal of Heavy Metals. *Environmental Nanotechnology, Monitoring and Management*, **12**; 100233

Vesali-Naseh, M., M. R. Vesali Naseh, and P. Ameri (2021). Adsorption of Pb (II) Ions from Aqueous Solutions Using Carbon Nanotubes: A Systematic Review. *Journal of Cleaner Production*, **291**; 125917

Wang, J. and X. Guo (2020). Adsorption Isotherm Models: Classification, Physical Meaning, Application and Solving Method. *Chemosphere*, **258**; 127–279

Wang, X., G. Wang, A. Marchetti, L. Wu, L. Wu, and Y. Guan (2019). Preparation of Porous Hydroxyapatite and Its Application in Pb Ions Effective Removal. *AIP Advances*, **9**(2)

Yan, S., W. Yu, T. Yang, Q. Li, and J. Guo (2022). The Adsorption of Corn Stalk Biochar for Pb and Cd: Preparation, Characterization, and Batch Adsorption Study. *Separations*, **9**(2); 1–13

Yang, M., L. Lin, B. Wang, Y. Wang, L. Zhang, Y. Jiang, M. Zhao, J. Zeng, H. Chen, and Y. Zhang (2021). A Facile Yet Versatile Method for Adsorption and Relayed Fluorescent Detection of Heavy Metal Ions. *Journal of Environmental Chemical Engineering*, **9**(4); 105737

